

V393  
.R46

Report 1844

MIT LIBRARIES



3 9080 02753 0275



DEPARTMENT OF THE NAVY

HYDROMECHANICS



AERODYNAMICS



STRUCTURAL  
MECHANICS



APPLIED  
MATHEMATICS

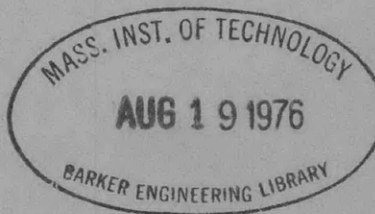


ACOUSTICS AND  
VIBRATION

THE EFFECT OF INTERMEDIATE HEAVY FRAMES ON THE ELASTIC  
GENERAL-INSTABILITY STRENGTH OF RING-STIFFENED  
CYLINDERS UNDER EXTERNAL HYDROSTATIC PRESSURE

by

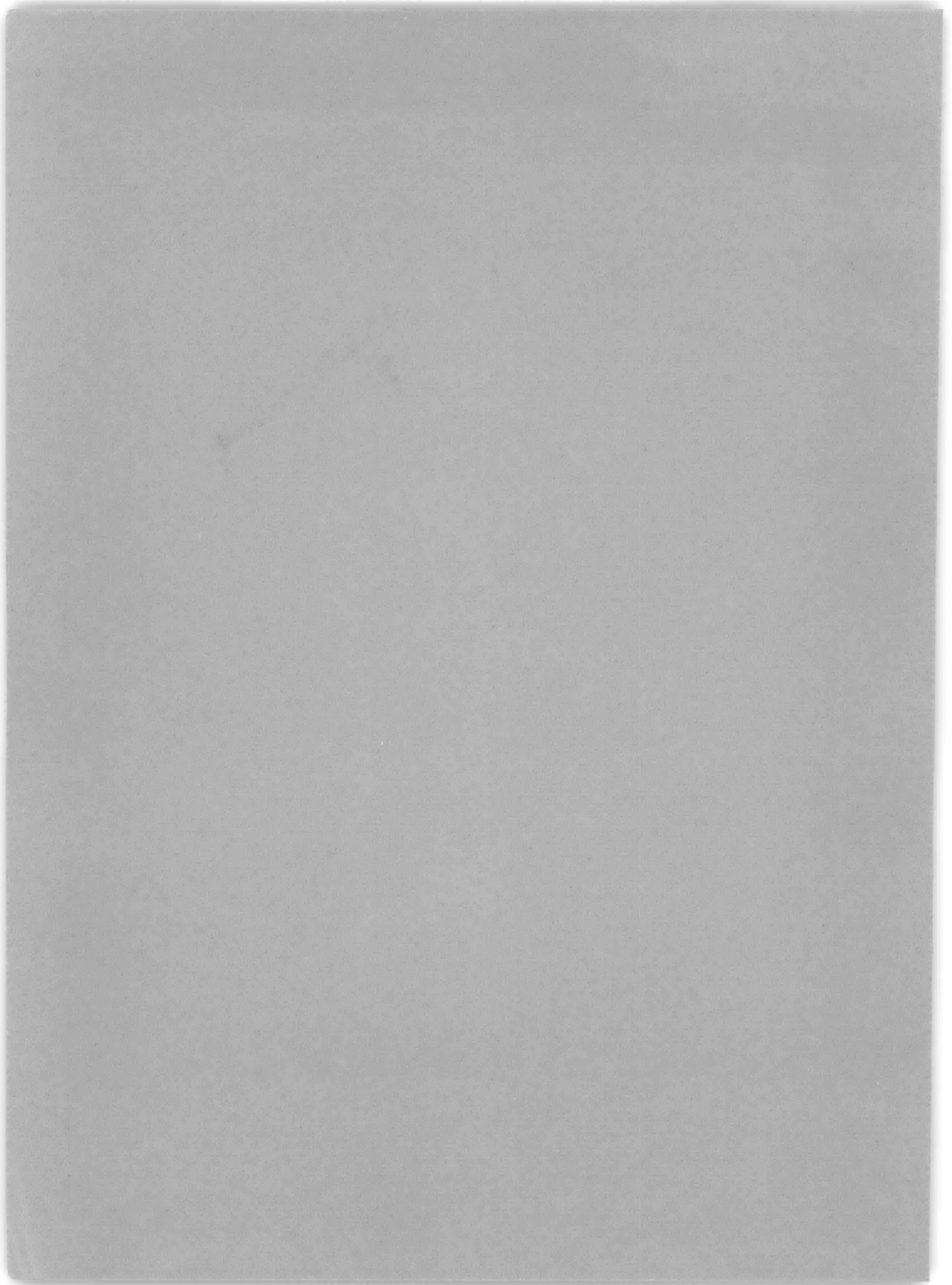
William F. Blumenberg



STRUCTURAL MECHANICS LABORATORY  
RESEARCH AND DEVELOPMENT REPORT

February 1965

Report 1844



THE EFFECT OF INTERMEDIATE HEAVY FRAMES ON THE ELASTIC  
GENERAL-INSTABILITY STRENGTH OF RING-STIFFENED  
CYLINDERS UNDER EXTERNAL HYDROSTATIC PRESSURE

by

William F. Blumenberg

February 1965

Report 1844

## TABLE OF CONTENTS

	Page
ABSTRACT .....	1
ADMINISTRATIVE INFORMATION .....	1
INTRODUCTION .....	1
DESCRIPTION OF MODELS .....	2
INSTRUMENTATION AND TEST PROCEDURE .....	7
TEST RESULTS AND DISCUSSION .....	11
WORK IN PROGRESS .....	23
CONCLUSIONS .....	24
REFERENCES .....	25

## LIST OF FIGURES

	Page
Figure 1 - Typical Stress-Strain Curve for 7075-T6 Aluminum Alloy .....	3
Figure 2 - Axial Sections of Ring-Stiffened Cylinders with Intermediate Heavy Frames .....	4
Figure 3 - Heavy-Frame Sections .....	6
Figure 4 - Test Apparatus .....	9
Figure 5 - Representative Experimental Pressure-Strain Plots .....	10
Figure 6 - Models after Failure .....	13
Figure 7 - Observed Circumferential Buckling Patterns .....	16
Figure 8 - Heavy-Frame-Effective-Shell Section .....	17
Figure 9 - Theoretical and Empirical Heavy-Frame Solutions Compared with Experimental Collapse Pressures .....	19
Figure 10 - Theoretical and Experimental Overall Collapse Pressures versus Length of Stiffened Cylinder .....	21
Figure 11 - Graphical Representation of Equation [2] .....	22

## LIST OF TABLES

	Page
Table 1 - Parameters of Heavy-Frame-Shell Sections .....	8
Table 2 - Experimental Results .....	12

## ABSTRACT

Twenty-four machined models were collapsed under external hydrostatic pressure to evaluate the effect of intermediate heavy frames on the elastic general-instability strength of ring-stiffened cylinders. The models were designed with various overall lengths, heavy-frame spacings, and heavy-frame sizes; the cylinder diameter, the shell thickness, and the typical-stiffener size and spacing were held constant.

The test results indicate that the effectiveness of a particular size of intermediate heavy frame decreases as the cylinder is lengthened at least to six diameters and also that the minimum size of heavy frames necessary to localize the failure between the heavy frames is possibly not dependent upon their spacing.

The values predicted by available analytical solutions show poor agreement with experimental results, whereas an existing empirical heavy-frame formula and a formula presented herein show better correlation.

It should be recognized that the models tested were designed in an extreme geometry range where the typical stiffener area was small in relation to the shell area and that further experimental investigation is necessary in cases where the typical frames are comparatively much larger, as in the hull structure of deep-diving submersibles.

## ADMINISTRATIVE INFORMATION

The investigation discussed in this report was carried out as part of the David Taylor Model Basin Submarine Structural Research program under Project S-F013 03 02, Task 1952.

## INTRODUCTION

The effectiveness of intermediate heavy frames in increasing the elastic general-instability strength of hydrostatically loaded, ring-stiffened cylinders is being investigated as a part of the David Taylor Model Basin Submarine Structural Research Program. This information is important for the efficient structural design of long compartments of deep-diving submersibles. No proven design methods or criteria are presently available for the design of this type of framing system.

Previous experimental results obtained from nondestructive tests of a machined ring-stiffened cylinder with a single heavy frame were reported

in Reference 1.\* These results indicated that a heavy frame can be an effective substitute for an internal bulkhead in increasing the elastic general-instability strength of a cylindrical pressure hull. Two heavy-frame solutions were presented, one an empirical solution based on the Lévy<sup>2</sup> ring formula and the other a modification of Kendrick's Part IV<sup>3</sup> analytical solution; these yielded results which were in close agreement with the experimental findings. However, it was stated in Reference 1 that the accuracy of the two solutions should be further investigated through destructive testing of small-diameter machined cylinders.

Twenty-four models were designed and tested to determine the effect of varying the cylinder length and the heavy-frame spacing, in addition to the heavy-frame strength, on the elastic overall collapse pressure. The experimental results are compared with the two heavy-frame solutions of Reference 1 and a solution presented herein.

#### DESCRIPTION OF MODELS

Determination of the elastic general-instability strength of submarine pressure hulls is difficult since the hulls are designed to fail by yielding of the structural material. Therefore, in order to check the validity of the heavy frame solutions in the elastic range, it was necessary to design the test cylinders with thick shells and light frames relative to submarine geometry so that the models would buckle elastically before yielding. Manufacturing the models of a material having a low modulus of elasticity and a high proportional limit relative to steel also raises the pressure at which yielding initiates and lowers the pressure at which the cylinder buckles.

The models reported herein were machined from 7075-T6 aluminum alloy bar stock (proportional limit = 60,000 psi; modulus of elasticity = 10,800,000 psi). A typical stress-strain curve obtained from a specimen of this material is shown in Figure 1.

The 24 models were divided into four groups; the typical dimensions of the models in Groups 1, 2, 3, and 4 are shown schematically in Figures

---

\*References are listed on page 25.

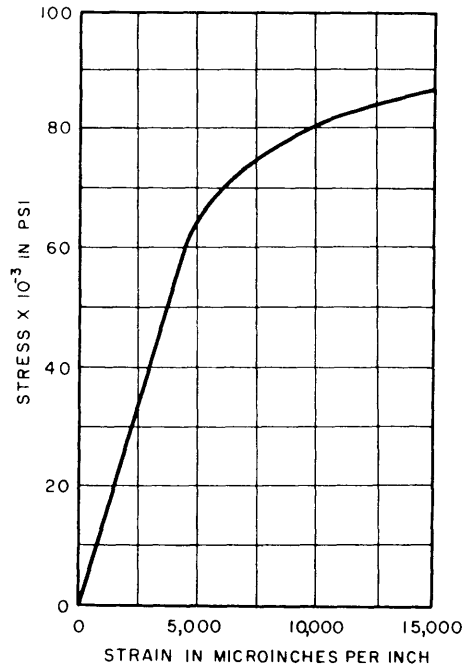


Figure 1 - Typical Stress-Strain Curve  
for 7075-T6 Aluminum Alloy

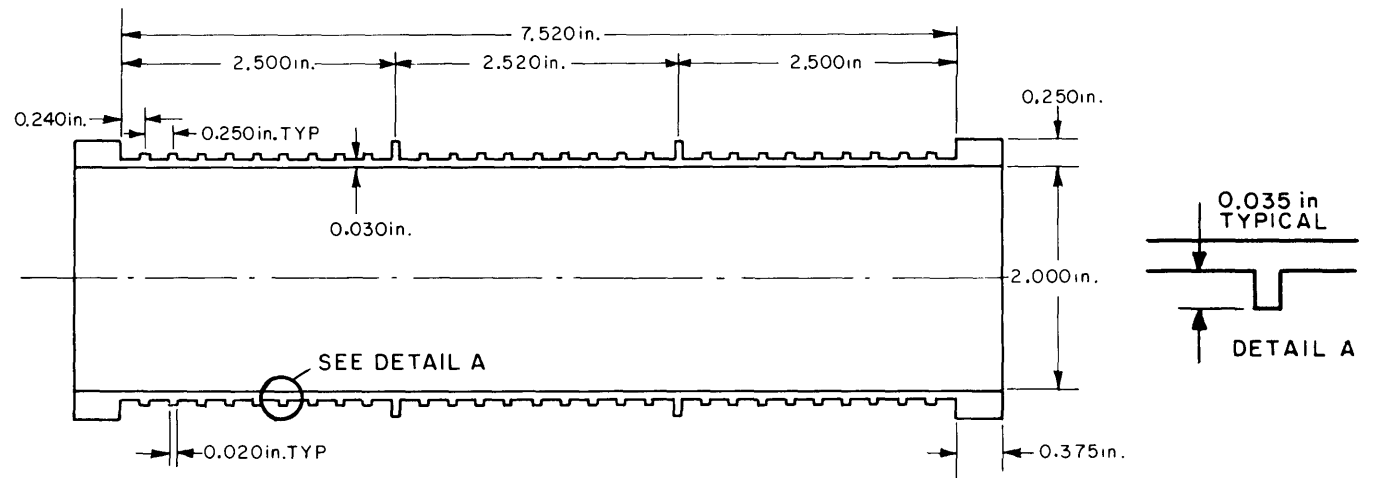
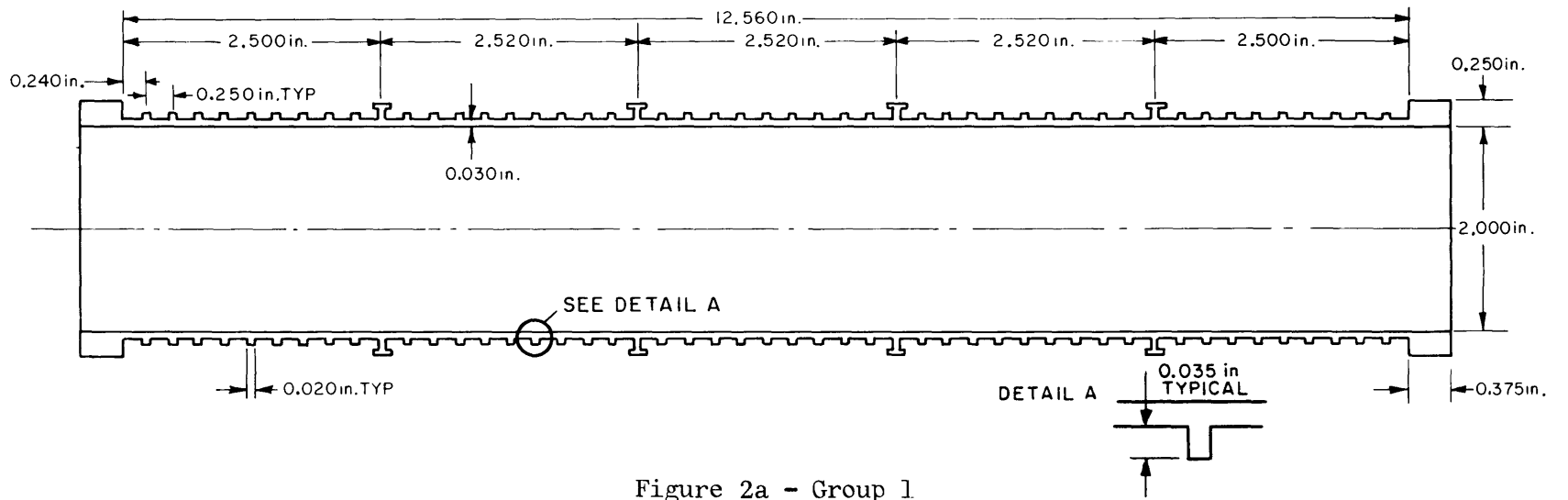
2a, b, c, and d, respectively. For each group, only the heavy-frame strength was varied, from model to model, from that for a typical stiffener up to that for a frame which was considered to be fully effective.\* The dimensions of the different heavy frames are shown in Figure 3. For simplicity of machining, the smaller heavy frames were made rectangular in shape. As they became deeper, some concern was felt that they might be prone to local crippling because of their low torsional resistance; therefore, the larger heavy frames were designed with a T-configuration for increased stability.

To investigate the effect of overall cylinder length on the elastic general-instability strength, the models in Groups 1, 2, and 3 were

---

\* A fully effective heavy frame is considered to be one which causes the failure to occur between, and not including, adjacent heavy frames.

Figure 2 - Axial Sections of Ring-Stiffened Cylinders with Intermediate Heavy Frames





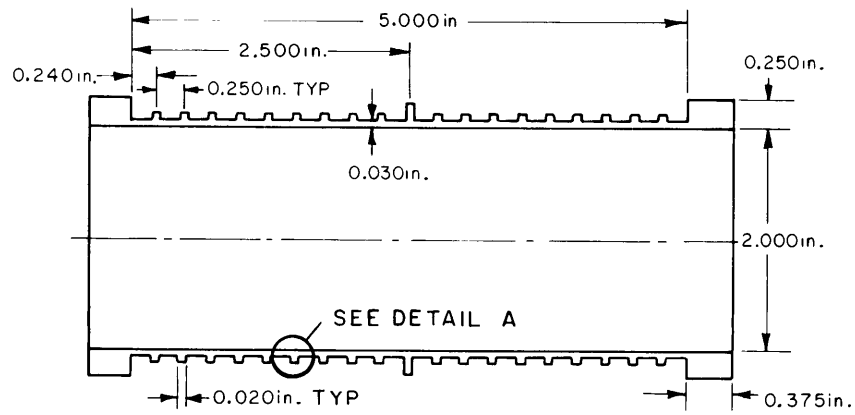


Figure 2c - Group 3

5

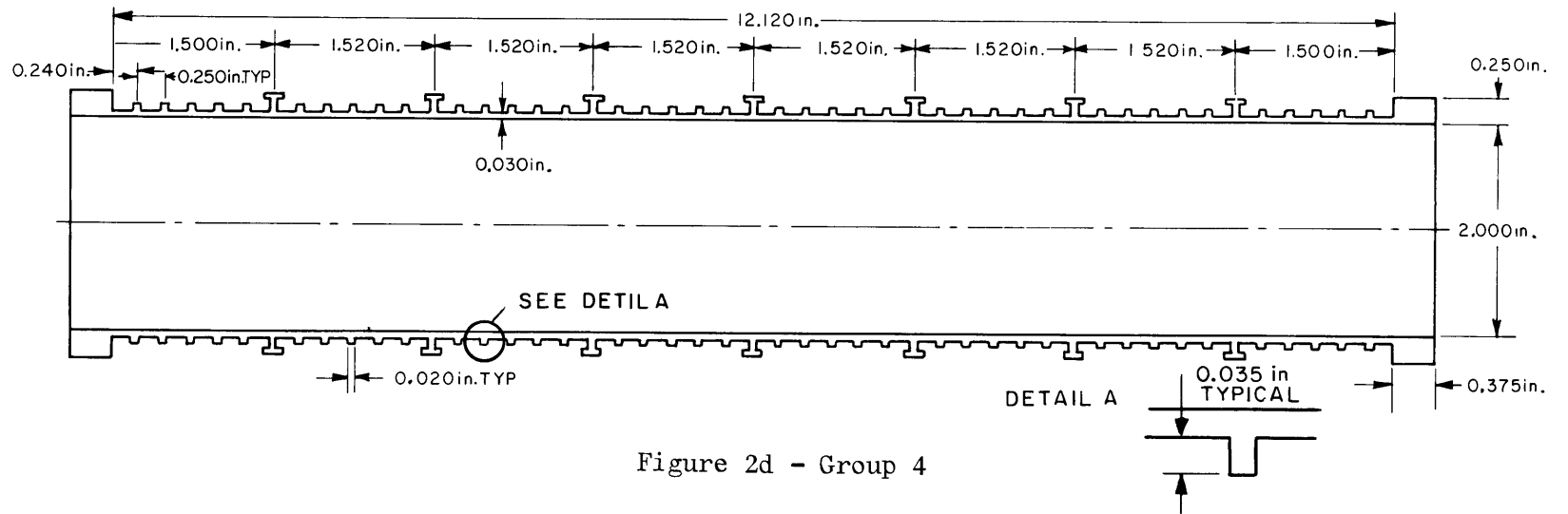


Figure 2d - Group 4

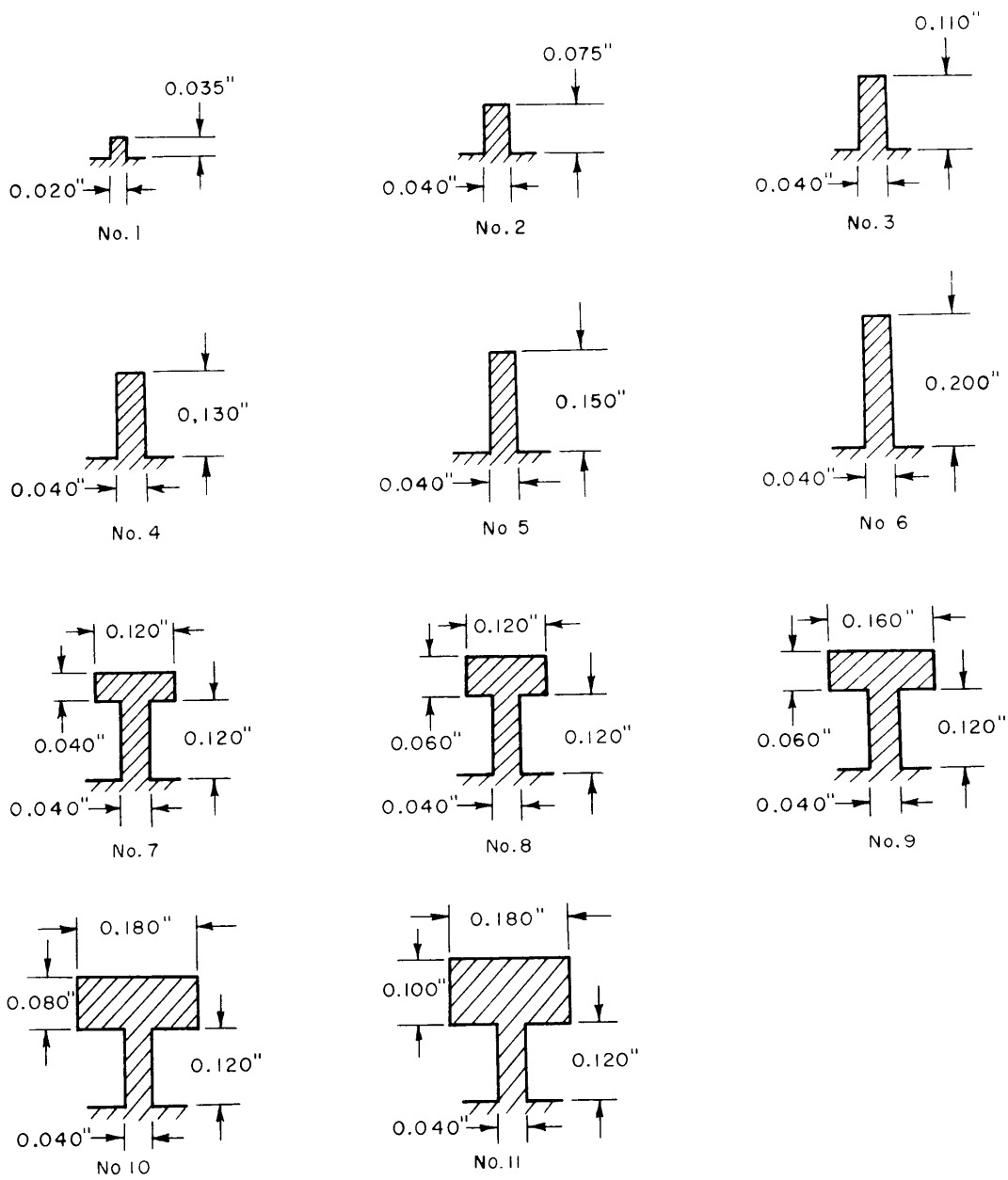


Figure 3 - Heavy-Frame Sections

designed with  $\frac{L_B^*}{R}$  ratios of 12.37, 7.41, and 4.93, respectively. The models in Group 4 were designed to determine the effect of the heavy-frame spacing on the elastic general-instability strength by a comparison between the test results of the Group 4 and the Group 1 models. The  $\frac{L_B}{R}$  ratio of 11.94 for the Group 4 models was approximately the same as that of the models in Group 1, but the heavy frames were spaced 40 percent closer. The geometry of the typically stiffened regions of the models was identical for the four groups. Table 1 lists each model with its appropriate grouping and type of heavy-frame section.

#### INSTRUMENTATION AND TEST PROCEDURE

The instrumentation consisted of electrical-resistance strain gages on the exterior surface of the models to determine the circumferential buckling patterns developed under hydrostatic load. Gages were located on the center-most heavy frame to determine the circumferential buckling pattern that extended over the full length of the model and on the shell to determine the circumferential buckling pattern that was localized between the heavy frames. In each grouping, the models with the strongest heavy frames were tested first to ensure that the frames were fully effective. The remaining models in each group were then tested in sequential order of decreasing heavy-frame strength. Once the buckling patterns of the models indicated that the heavy frames were less than fully effective, the subsequent models were tested to failure without instrumentation.

The model ends were closed with thick plates which were inserted into the ends and sealed with O-rings (see Figure 4). Lead wires (single-strand magnet wire) from the strain gages were strung through a hole in the tank closure head and sealed in place with epoxy resin. Heavier stranded hook-up wire was then used to complete the circuit with the recording equipment. The volume of the test chamber was reduced by means of

---

$\frac{L_B^*}{R}$  is the distance between end rings divided by the cylinder radius to the midplane of the shell.

TABLE 1  
Parameters of Heavy-Frame-Shell Sections

Model Number	Group Number	Heavy-Frame Section Number	$L_{Fe}^{**}$ in.	$e_F$ in.	$e_{FSe}$ in.	$I_{FSe}^{\dagger}$ $\times 10^{-6}$ in.	$\frac{I_{FSe}^{\dagger\dagger}}{I_{fse}}$
1	1	1	0.260	0.033	0.003	1.33	1.00
2	1	2	0.214	0.053	0.017	7.53	5.66
3	1	3	0.195	0.070	0.030	17.18	12.92
4	1	4	0.186	0.080	0.039	24.94	18.75
5	1	5	0.177	0.090	0.048	34.48	25.92
6	1	6	0.160	0.115	0.072	66.44	49.95
7	1	7	0.149	0.115	0.078	62.49	46.98
8	1	8	0.136	0.129	0.096	82.31	61.89
9	1	9	0.126	0.135	0.107	89.41	67.23
10	1	10	0.111	0.150	0.128	113.49	85.33
11	1	11	0.103	0.162	0.143	137.93	103.71
12	2	1	0.260	0.033	0.003	1.33	1.00
13	2	3	0.195	0.070	0.030	17.18	12.92
14	2	5	0.177	0.090	0.048	34.48	25.92
15	2	6	0.160	0.115	0.072	66.44	49.95
16	3	1	0.260	0.033	0.003	1.33	1.00
17	3	2	0.214	0.053	0.017	7.53	5.66
18	3	3	0.195	0.070	0.030	17.18	12.92
19	3	4	0.186	0.080	0.039	24.94	18.75
20	3	5	0.177	0.090	0.048	34.48	25.92
21	4	5	0.177	0.090	0.048	34.48	25.92
22	4	7	0.149	0.115	0.078	62.49	46.98
23	4	9	0.126	0.135	0.107	89.41	67.23
24	4	10	0.111	0.150	0.128	113.49	85.33

\*See Figure 3

\*\*See Equation [1]

$I_{FSe}^{\dagger}$  is moment of inertia of heavy-frame-effective-shell section about its centroid.

$I_{fse}^{\dagger\dagger}$  is moment of inertia of typical-frame-effective-shell section about its centroid.

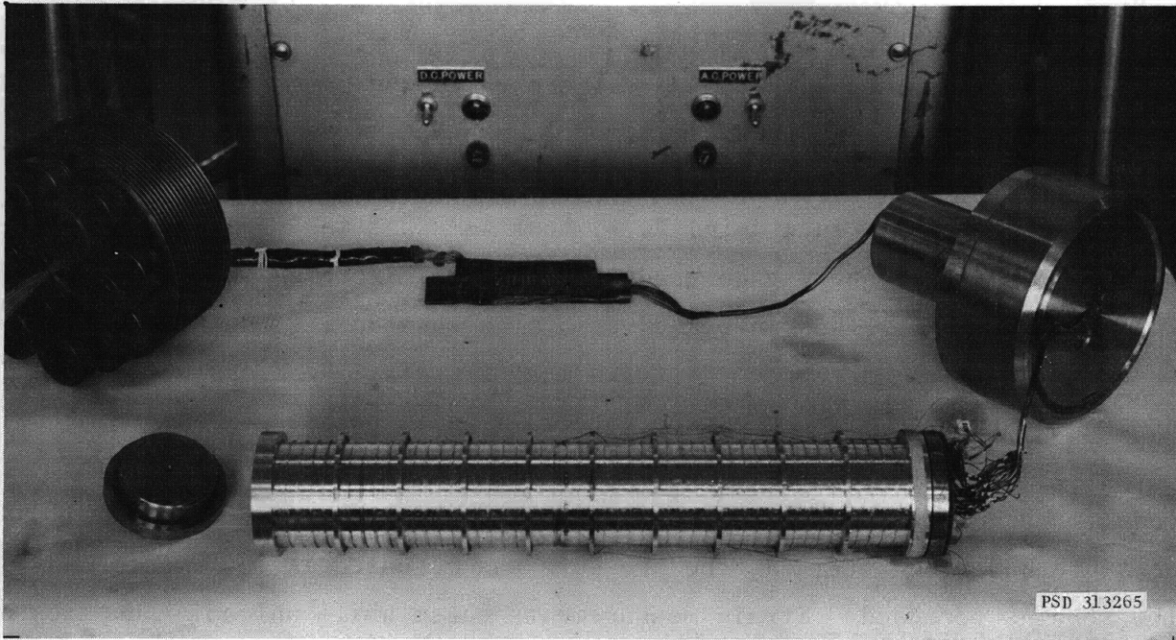


Figure 4a - Model Prepared for Test

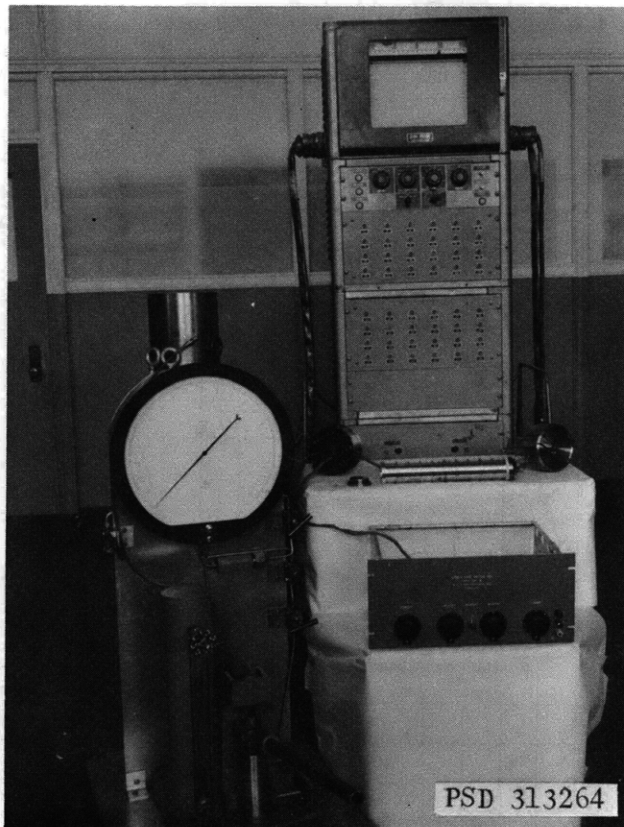


Figure 4b - Pressure Tank System and Recording Equipment

Figure 4 - Test Apparatus

filler blocks to reduce the amount of energy in the pressurizing fluid at the time of failure and thus limit model damage to a distinguishable buckling pattern. Each cylinder was loaded externally, with oil as the pressurizing medium, in a 4-in. I. D. test tank and the pressure was measured by a laboratory gage graduated in 1-psi increments.

The pressure was increased at a slow rate during the test run with frequent 2-min holds to record strain measurements. Readings were taken at progressively smaller pressure intervals as it became evident from the observed strain that large buckling deformations were developing in the model. When it was estimated that approximately 98 percent of the collapse pressure had been attained, the pressure was released in increments and the strains recorded. Strain measurements taken while unloading duplicated those measured during the loading cycle, thus indicating that the observed deformations were elastic. Representative pressure-strain plots of the first pressure run for gages on the heavy frames of Models 23 and 24 are shown in Figure 5. For both models, the strain plot for Gage 1 indicates

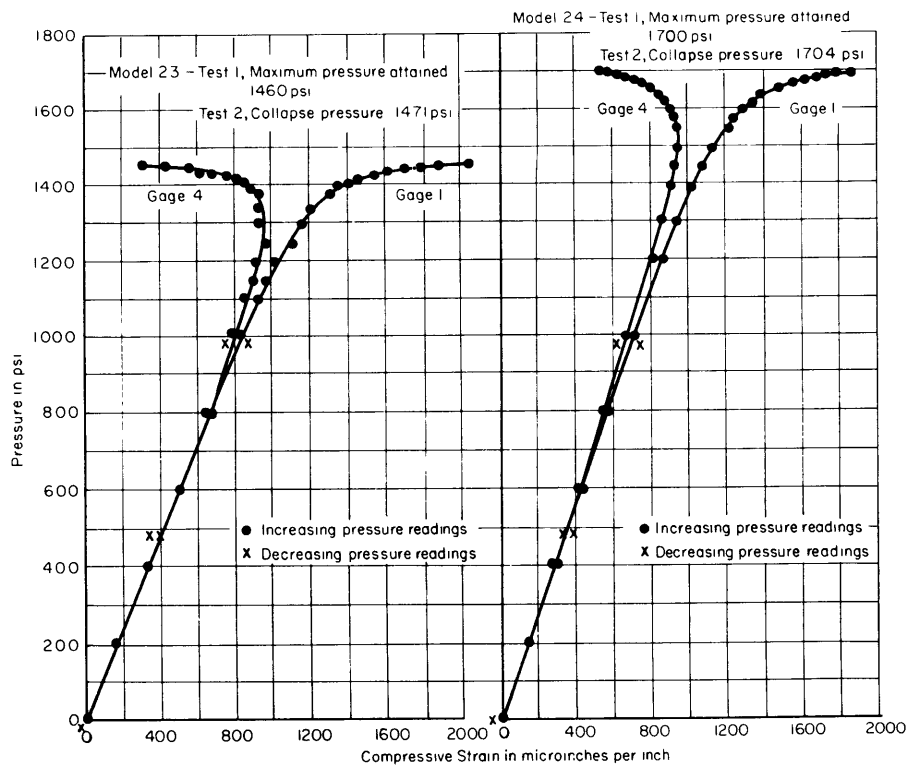


Figure 5 - Representative Experimental Pressure-Strain Plots

that this location was moving radially inward relative to the axisymmetric deflection while the location at Gage 4 was moving radially outward relative to the same reference. In a second test run, pressure was increased until the model collapsed. Models without instrumentation were tested to failure in one run; the loading rate was approximately the same as that for the instrumented models.

## TEST RESULTS AND DISCUSSION

The experimental collapse pressures and the observed buckling modes obtained from the model tests are listed in Table 2; photographs of the models after failure are shown in Figure 6. In some instances, the apparent damage to the models implied failure between heavy frames. However, examination of the strain measurements indicated that the collapse modes were overall and the local damage was a result of the post-buckling behavior. For instance, Figure 6a shows Model 9 with the visible damage limited to the region between the two center-most heavy frames. The maximum circumferential strain distribution recorded for Model 9 during the second test run (Figure 7a) indicates that a high degree of bending of the heavy frame had existed in a two-lobe buckling pattern. The shell strain distribution was also in a two-lobe pattern and was in phase with that of the heavy frame; i.e., for each generator around the circumference of the model, the heavy frame and the shell were buckling in the same direction (overall buckling pattern). If the heavy frames of Model 9 had been fully effective, strain distribution patterns such as that shown in Figure 7b (Model 10) would have been observed. The maximum recorded strain distribution around the heavy frame of Model 10 was also in a two-lobe pattern but showed only a small degree of bending, while the shell strain distribution indicated that a larger degree of bending had existed at this location in a four-lobe buckling pattern.

Listed in Table 1 are the computed values of the effective moment of inertia (taken about the longitudinal centroidal axis and reflecting the circumferential bending rigidity of the structure) of the heavy frame-shell section that includes the heavy stiffener plus an effective width of shell, as shown in the schematic diagram of Figure 8. The effective width of shell acting with each frame on a uniformly ring-stiffened

TABLE 2  
Experimental Results

Model Number	Collapse Pressure psi	Mode of Failure	
		n*	Longitudinal Buckling Pattern
1	240	2	Overall
2	299	2	↓
3	407	2	
4	464	2	
5	555	2	
6	795	2	
7	777	2	
8	913	2	
9	963	2	
10	1055	4	
11	1020	4	Between heavy frames
12	480	3	Overall
13	785	3	↓
14	948	3	
15	1048	4	Between heavy frames
16	621	3	Overall
17	797	3	↓
18	967	3	
19	1063	3	
20	1075	4	Between heavy frames
21	758	2	Overall
22	1115	2	↓
23	1471	2	
24	1704	5	Between heavy frames

\* n is the number of circumferential buckling lobes.



Figure 6 - Models after Failure

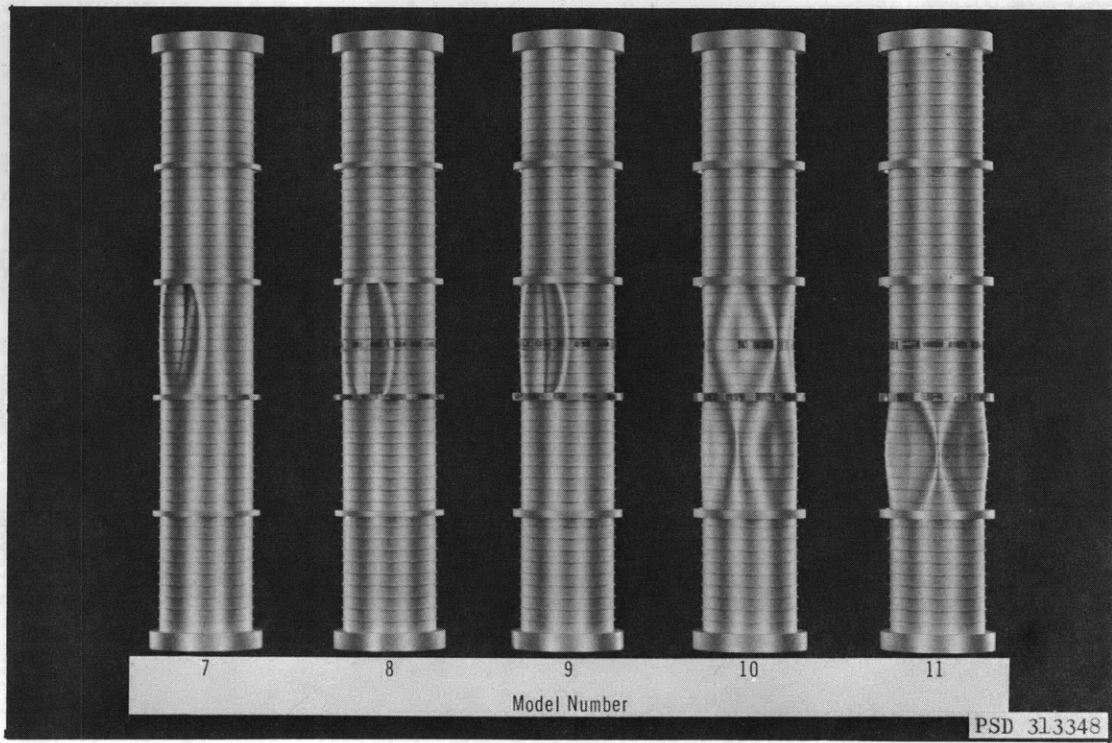
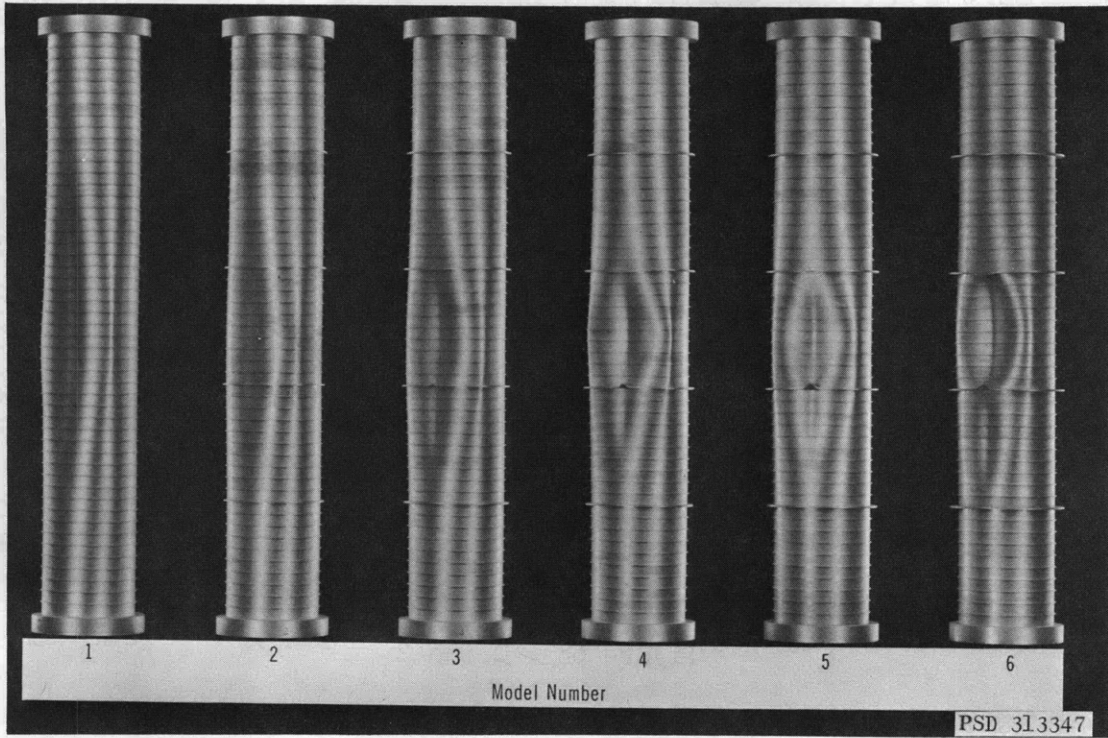


Figure 6a - Group 1

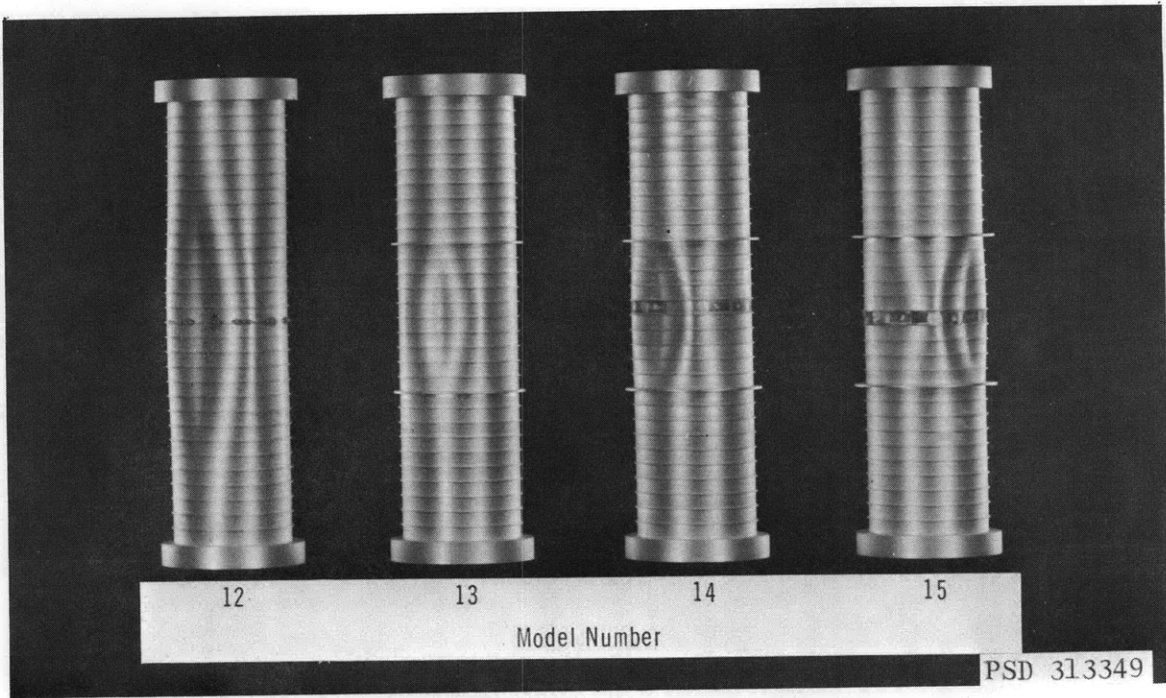


Figure 6b - Group 2

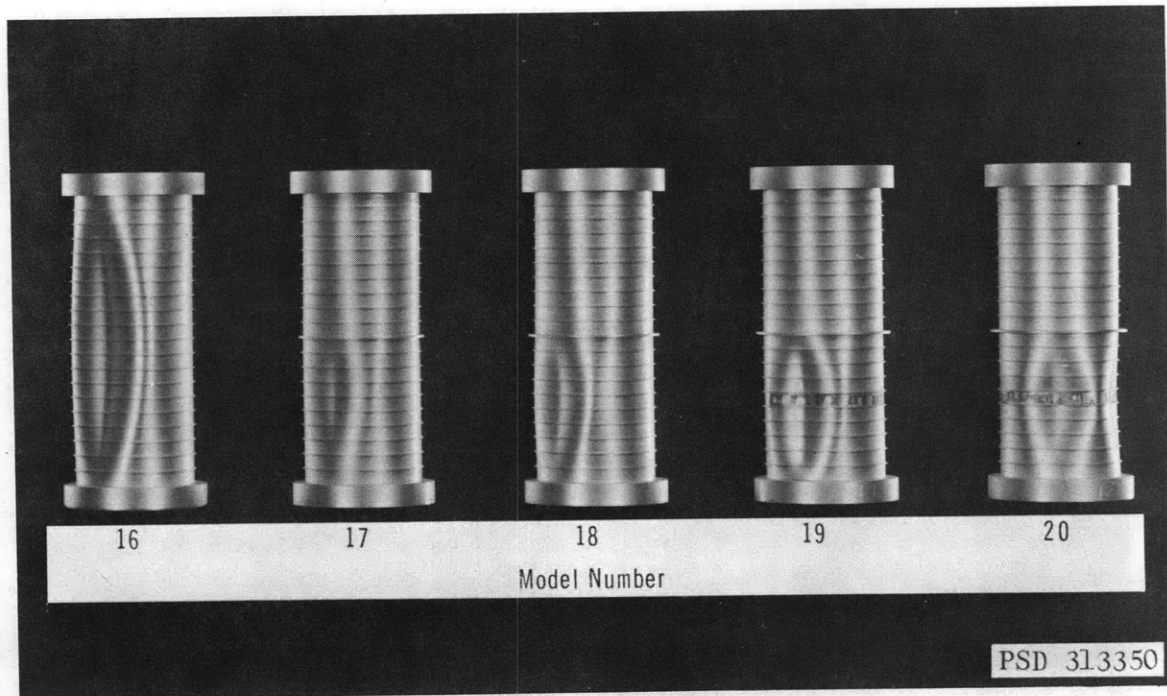


Figure 6c - Group 3

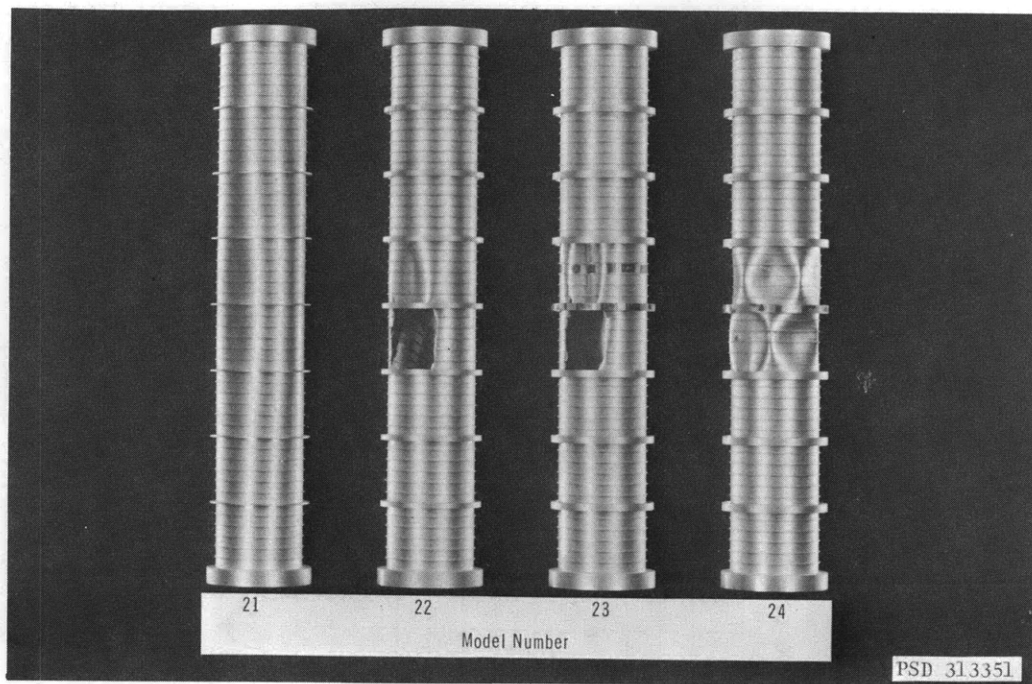


Figure 6d - Group 4

cylinder, as used in the frame stiffness parameter in Reference 4, is equal to  $\ell F_1 + b$ ,

where  $\ell$  is the unsupported width of shell between frames,  
 $F_1$  is a function defined by Equation [72],<sup>4</sup> and  
 $b$  is the faying or web width of the ring frames in contact with the shell.

Sequential increases in the strength of evenly spaced intermediate frames on the uniformly stiffened cylinder will cause increasingly more longitudinal bending of the shell at these locations and subsequently reduce the effective width of shell acting with the strengthened frame to resist circumferential buckling. This reduction in width can be approximated by using a ratio of the combined cross-sectional area of a typical frame and a typical bay width of shell ( $A_{fs}$ ) to that of the strengthened (heavy) frame and its bay width of shell ( $A_{FS}$ ) so that the effective width of shell acting with the heavy frame is

$$L_{Fe} = \ell F_1 \left( \frac{A_{fs}}{A_{FS}} \right) + b \quad [1]$$

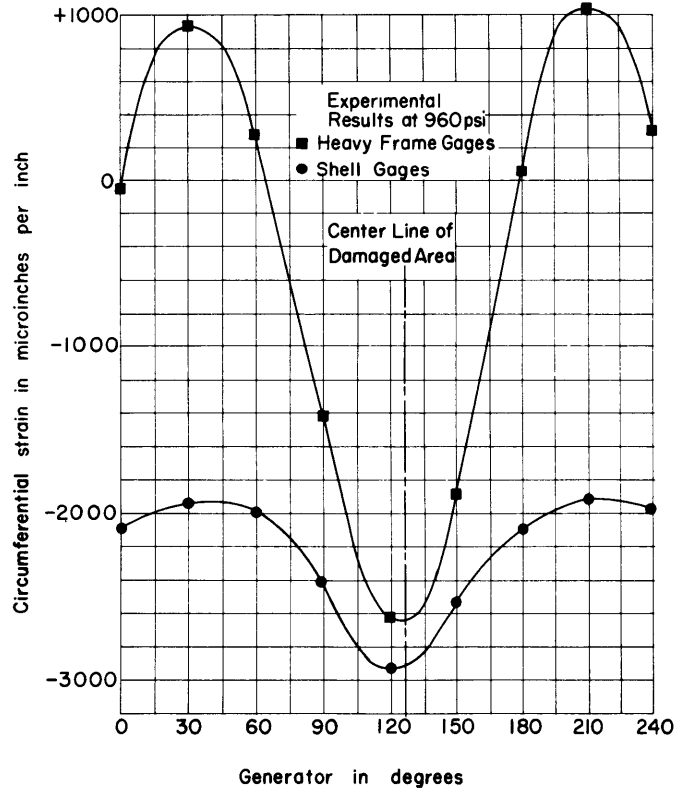


Figure 7a - Model 9

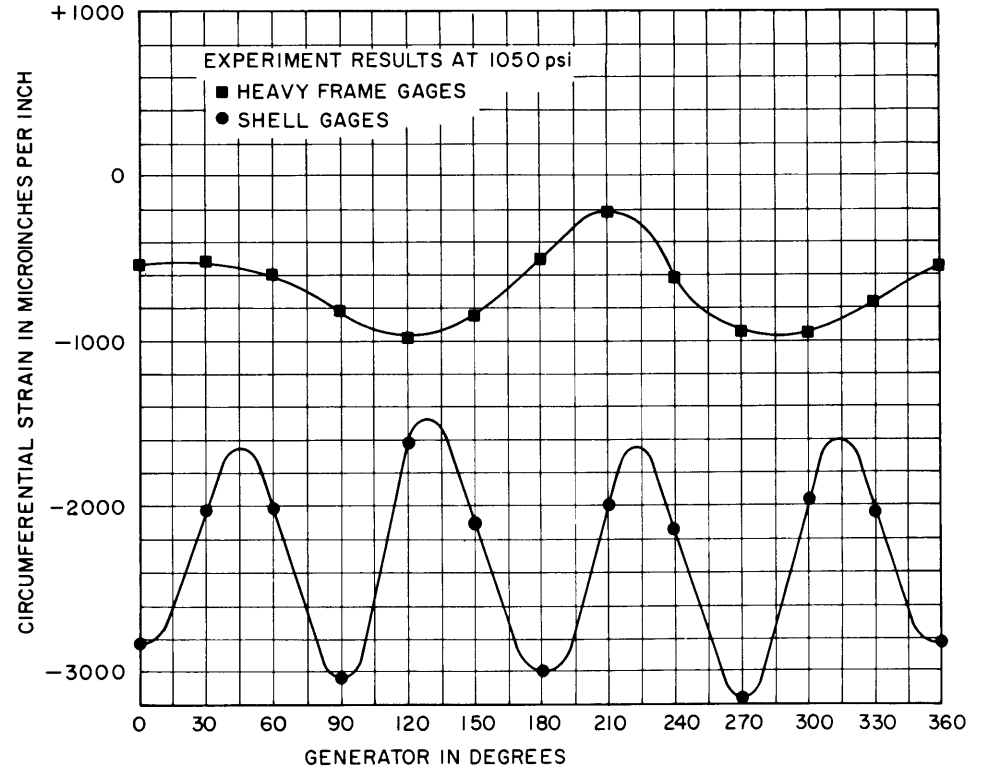
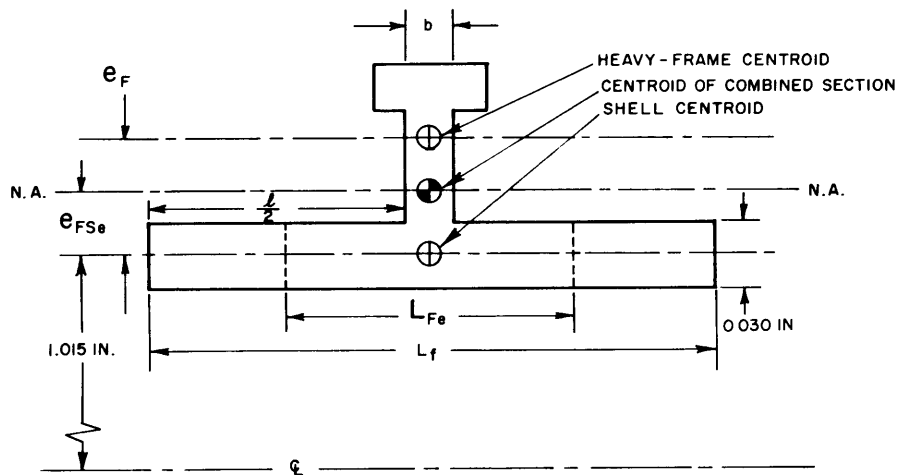


Figure 7b - Model 10

Figure 7 - Observed Circumferential Buckling Patterns



- $e_F$  IS DISTANCE FROM CENTROID OF SHELL TO CENTROID OF FRAME
- $e_{FS_e}$  IS DISTANCE FROM CENTROID OF SHELL TO CENTROID OF FRAME-EFFECTIVE-SHELL SECTION
- $L_{Fe}$  IS AN EFFECTIVE WIDTH OF SHELL
- $L_f$  IS THE CENTER-TO-CENTER SPACING OF THE TYPICAL FRAMES
- $l$  IS THE UNSUPPORTED WIDTH OF SHELL
- $b$  IS THE FAYING FLANGE OR WEB WIDTH

Figure 8 - Heavy-Frame-Effective-Shell Section

Using the effective width concept, the test results are represented graphically, for Groups 1, 2, 3, and 4, in Figures 9a, b, c, and d, respectively, where the abscissa is the ratio of the effective moment of inertia of the heavy-frame-shell section ( $I_{FS_e}$ ) to that of the effective moment of inertia of the typical-frame-shell section ( $I_{fse}$ ). A significant observation made in comparing the experimental results of Groups 1, 2, and 3 is that the strength required for a heavy frame to be fully effective increases as the cylinder is lengthened at least to 6 diameters (all other parameters held constant). For the particular model geometry tested, cylinder lengths ( $L_B$ ) of  $2 L_F^*$ ,  $3 L_F$ , and  $5 L_F$  required  $\frac{I_{FS_e}}{I_{fse}}$  values of at least 18.5, 37.0, and 78.0, respectively, to cause buckling between heavy frames. These results indicate that a 322 percent increase in the moment of inertia of the heavy frames is required to maintain a constant general-instability pressure if the model is lengthened 150 percent. Figure 10 illustrates the manner in which the critical pressure varies with cylinder length for a particular heavy-frame size. The solid line curves show how

---

\* $L_F$  is the heavy-frame spacing.

the general-instability pressure and the circumferential buckling mode predicted by the theory of Reference 5 will vary with overall length for cylinders with all typical frames and of the same geometry as the models tested. The circle points representing the experimental results of Models 1, 12, and 16 (No. 1 size heavy frame is equal to the typical frame size) are connected with a dotted line curve of the same character as the theoretical curve to show how the experimental collapse pressures compare with the theoretical results of Reference 5. Strengthening the frame slightly at the heavy-frame locations causes the curve to move upward, as indicated by the dotted line drawn through the square points, which are the experimental results of Models 3, 13, and 18 (No. 3 size heavy frame). Successive increases in frame strength at the heavy-frame locations will continue to displace the collapse pressure curves upward as indicated by the dotted lines for the No. 4 and No. 5 size heavy frames.

Model 7 was designed with T-frames (No. 7 heavy-frame section) which had approximately the same effective moment of inertia ( $I_{FSe}$ ) as the rectangular heavy frames of Model 6 but possessed much greater torsional restraint. The test results revealed (Figure 9a) that both frame configurations were equally effective in restraining overall instability, thus confirming that the effective moment of inertia is a fundamental buckling parameter.

Comparison of the test results in Figure 9a with those in Figure 9d reveals that the minimum size of heavy frame necessary to be fully effective may not be dependent upon the heavy-frame spacing for models of the same overall length. For these two model series, in which the models were of approximately the same overall length but had a 40 percent difference in the heavy-frame spacing, the  $\frac{I_{FSe}}{I_{fse}}$  ratios for a minimum size, fully effective, heavy frame were essentially the same (78.0 for the Group 1 cylinders and 80.5 for the Group 4 cylinders). Also presented in Figure 9 are the curves obtained by using an analytical heavy-frame solution.<sup>1</sup> Figures 9b and 9c substantiate the statement in Reference 1 that a shortcoming in the analytical heavy-frame solution often results in the erroneous appearance of the second mode as the overall critical buckling pattern. The predicted  $n = 2$  overall buckling pattern was not observed as the critical mode of

Figure 9 - Theoretical and Empirical Heavy-Frame Solutions Compared with Experimental Collapse Pressures

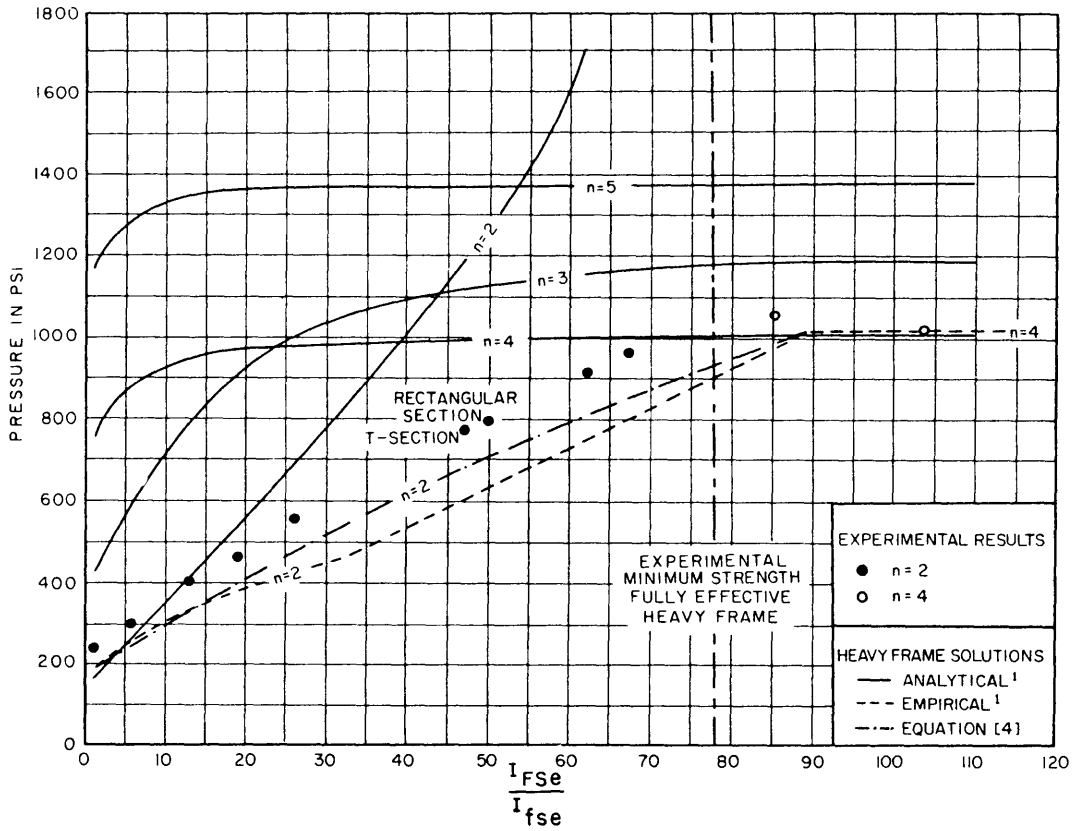


Figure 9a - Group 1

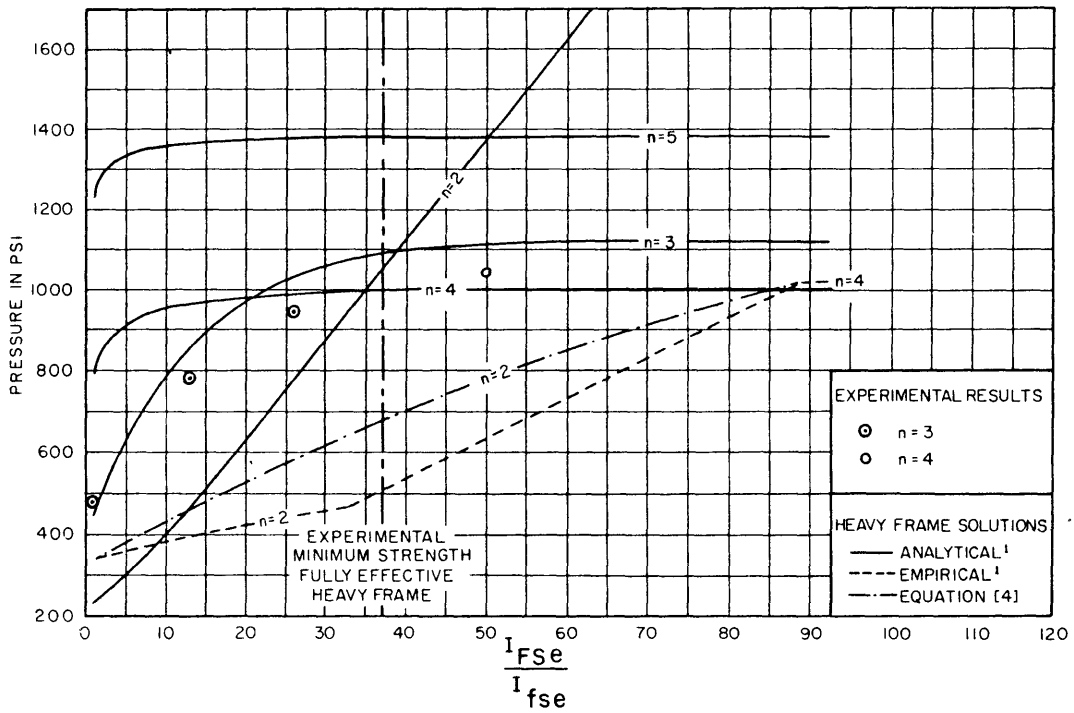


Figure 9b - Group 2

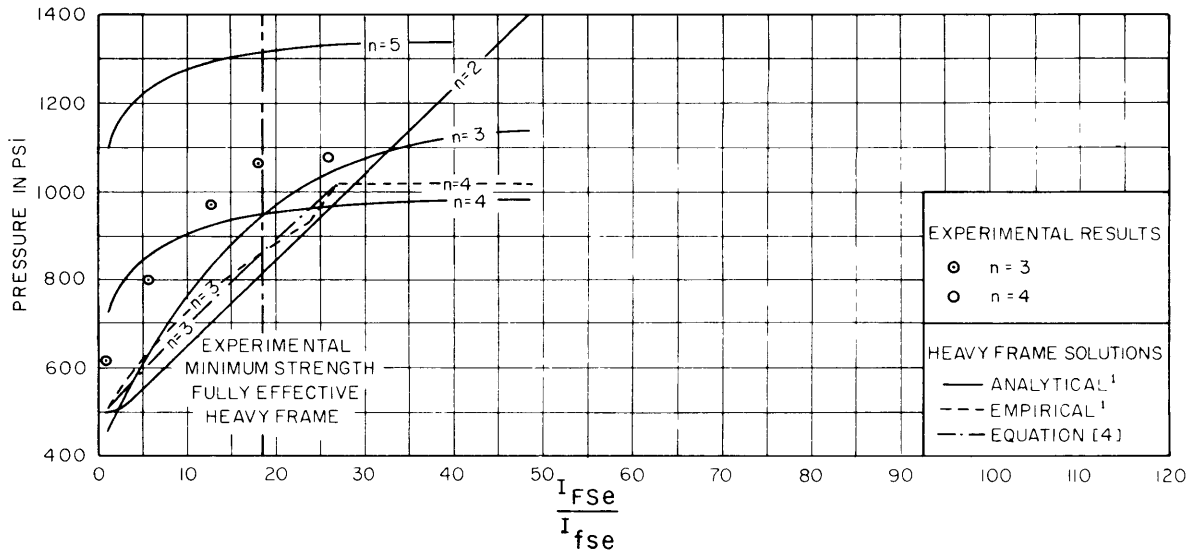


Figure 9c - Group 3

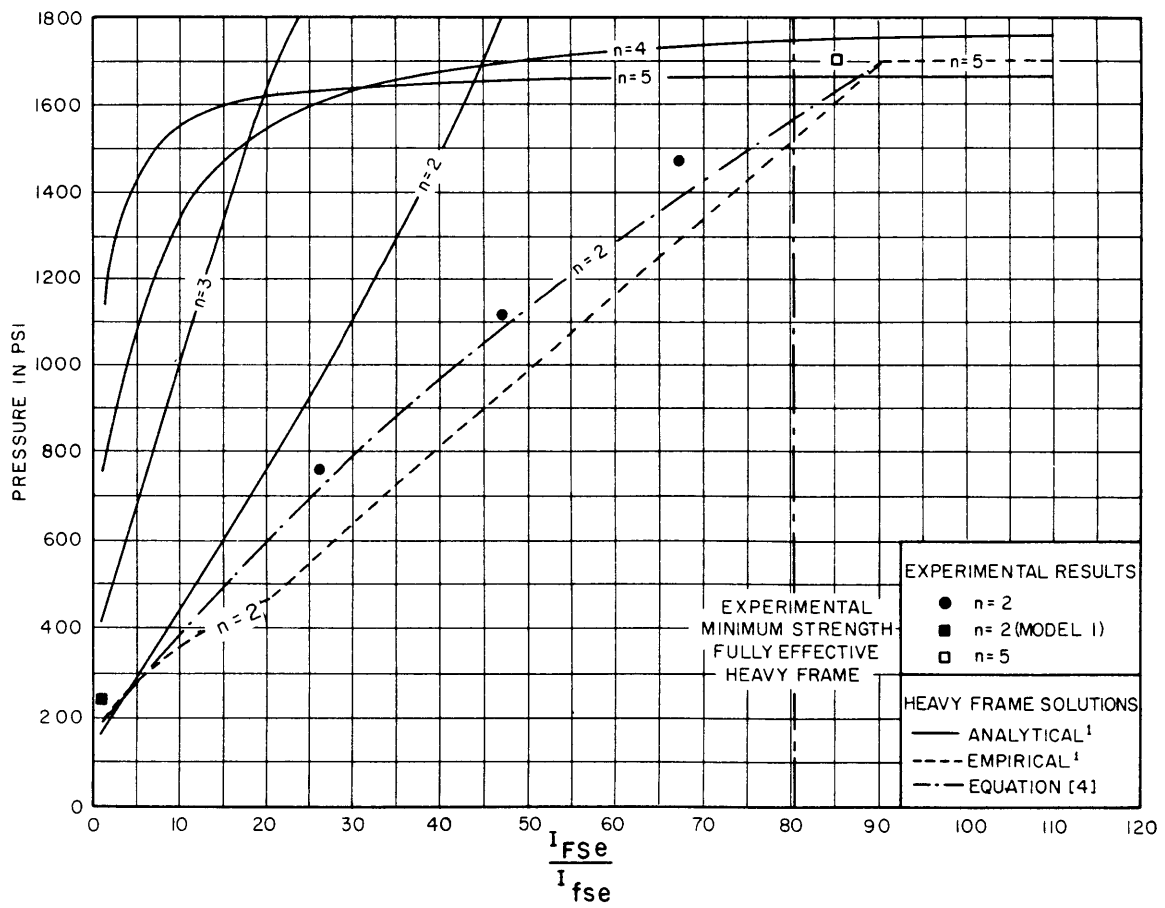


Figure 9d - Group 4



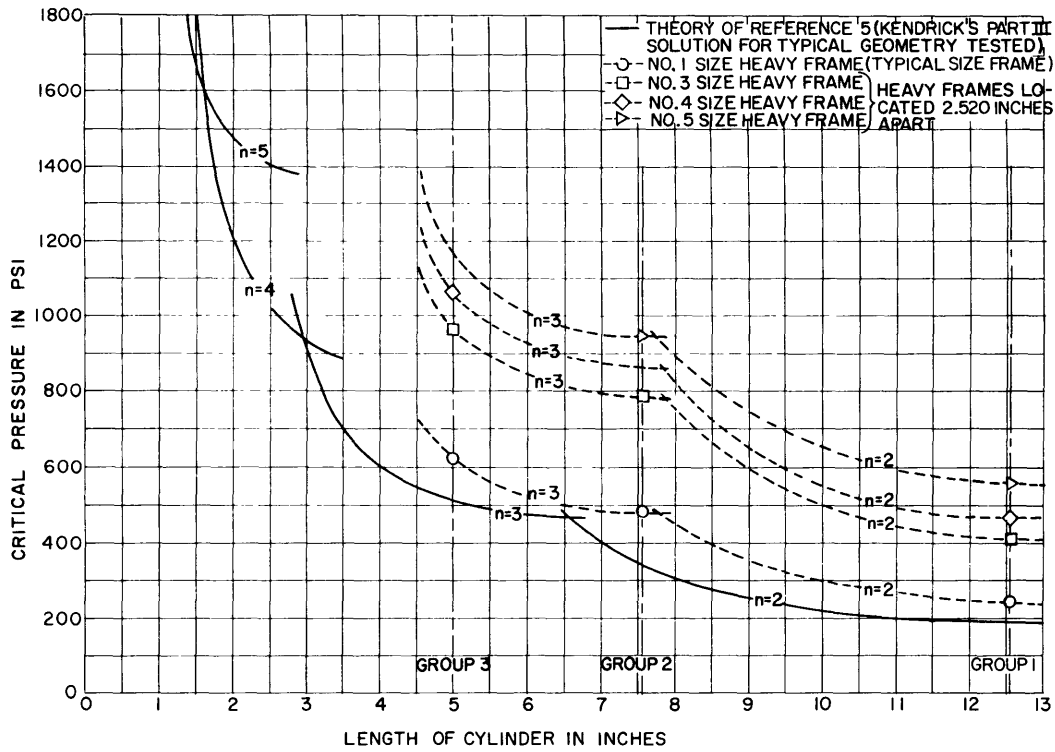


Figure 10 - Theoretical and Experimental Overall Collapse Pressures versus Length of Stiffened Cylinder

failure for the models in Groups 2 and 3; the models failed in an  $n = 3$  overall mode. Figures 9a and 9d indicate that when the heavy frames are less than fully effective, agreement between analytical and experimental results for the longer length models is good only where the heavy frame is slightly larger than typical. In all cases, the theory closely predicts the pressure that can be realized when failure occurs between heavy frames, that is, when the heavy frames are fully effective, but the estimate of the minimum size heavy frame required to initiate this type of failure is poor.

The dotted lines in Figure 9 represent values determined by the empirical heavy-frame formula<sup>1</sup> in which the required pressure terms were determined by Kendrick's Part III solution.<sup>5</sup> The agreement between the empirical solution and the experimental results is shown to be good in Figures 9a, c, and d. However, the values predicted for the models of Group 2 (Figure 9b) agree poorly with the test results due to an incorrect buckling mode determined by the theory of Reference 5; the incorrect value was  $n = 2$  (see Figure 10) whereas  $n = 3$  was found experimentally.

A better estimation than that of the empirical solution<sup>1</sup> can be

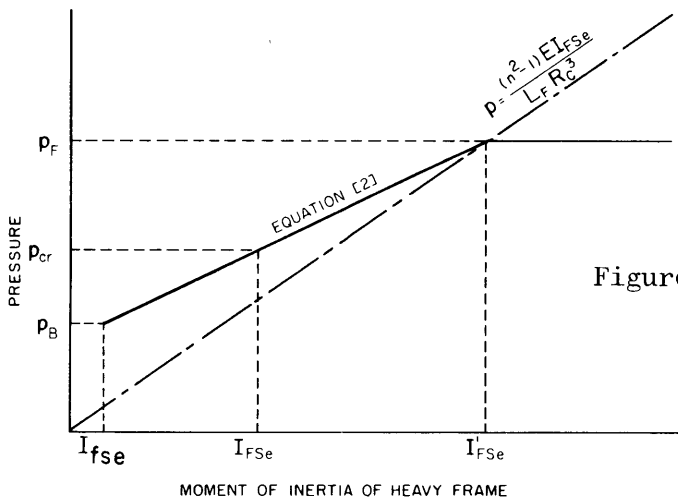


Figure 11 - Graphical Representation of Equation [2]

made of the test results by the following relationship:

$$p_{cr} = \frac{(I_{FSe} - I_{fse})}{(I'_{FSe} - I_{fse})} (p_F - p_B) + p_B \quad [2]$$

where  $I'_{FSe} \geq I_{FSe} \geq I_{fse}$  (see Figure 11), and where

$p_{cr}$  is the critical pressure for elastic general-instability failure of the cylinder,

$I_{FSe}$  is the moment of inertia of the heavy frame plus an effective width of shell (Equation [1]),

$I_{fse}$  is the moment of inertia of the typical frame plus an effective width of shell (Equation [1]),

$p_B$  is the critical pressure for elastic general-instability failure of the cylinder with the heavy frames replaced with typical frames,

$p_F$  is the critical pressure for elastic general-instability failure of the uniformly stiffened cylinder of length equal to the heavy frame spacing (this is the maximum pressure obtainable for a stiffened cylinder with intermediate heavy frames because the failure will continue to occur between the heavy stiffeners as their strength is increased further), and

$I'_{FSe}$  is the moment of inertia of the minimum strength fully effective heavy frame.

The value of the minimum strength fully effective heavy frame can be approximated by

$$I'_{FSe} = \frac{\sqrt[3]{p_F} \sqrt[3]{L_F} \sqrt[3]{R_c^3}}{(n^2 - 1) E} \quad [3]$$

where  $L_F$  is the heavy-frame spacing,

$R_c$  is the radius from the axis of the cylinder to the centroid of the effective heavy-frame-shell section,

$n$  is the critical buckling mode determined for  $p_B$ , and

$E$  is the modulus of elasticity of the material.

Combining Equations [2] and [3] results in

$$p_{cr} = \frac{(I_{FSe} - I_{fse}) (p_F - p_B)}{\frac{p_F L_F R_c^3}{(n^2 - 1)E} - I_{fse}} + p_B \quad [4]$$

The value of  $p_B$ ,  $p_F$ , and  $n$  can be determined with reasonable accuracy by using the graphical solution of Reference 4. It can be seen for each group in Figure 9 that the curve determined by Equation [4] agrees well with the experimental results especially for cylinders over four diameters in length (the discrepancy in Figure 9b is due to the erroneous prediction of the buckling mode as explained earlier in the text).

#### WORK IN PROGRESS

At the present the program utilizing the destructive testing of small-diameter machined cylinders is being continued to fully determine the effect of intermediate heavy frames on the general-instability strength of ring-stiffened cylinders, and to further evaluate the existing heavy-frame solutions. Interest is especially directed to the range of geometry where the dominating contribution to the general-instability strength is from large typical frames and not the shell, as in present-day deep submersibles. The theoretical investigation of the heavy-frame effect has been intensified.

The testing program has been expanded to determine if there is any advantage in using mixed intermediate framing, e.g., large heavy frames spaced alternately with medium-sized heavy frames, in lieu of all uniformly sized heavy frames.

## CONCLUSIONS

1. The effectiveness of a particular size of intermediate heavy frame in increasing the elastic general-instability strength of hydrostatically loaded ring-stiffened cylinders decreases as the cylinder is lengthened at least to six diameters.
2. Indications are that the minimum size of the intermediate heavy frames necessary to cause a ring-stiffened cylinder to fail between heavy frames is possibly not dependent upon the heavy-frame spacing.
3. Poor agreement exists between the experimental results and the values predicted by the analytical solution of Reference 1 for all models except those with extremely large intermediate heavy frames.
4. The empirical heavy-frame formula<sup>1</sup> and Equation [4] presented herein are the most practical and accurate methods known by the author for predicting the behavior of a ring-stiffened cylindrical shell with intermediate heavy frames. Equation [4] is the more acceptable of the two by reason of its greater accuracy and the ease with which it may be solved. Additional experimental results are necessary for a more complete evaluation.

## REFERENCES

1. Blumenberg, W. F. and Reynolds, T. E., "Elastic General Instability of Ring-Stiffened Cylinders with Intermediate Heavy Frames under External Hydrostatic Pressure," David Taylor Model Basin Report 1588 (Dec 1961).
2. Lévy, M., "Mémoire sur un nouveau cas intégrable du problème de l'élasticité et l'une de ses applications," Journal de math. pure et appl. (Liouville), Ser 3 to 10, pp. 5-24 (1884).
3. Kendrick S., "The Buckling under External Pressure of Circular Cylindrical Shells with Equally Spaced Circular Ring Frames-Part IV," Naval Construction Research Establishment Report R372 (Jul 1957).
4. Ball, W. E., "Formulas and Curves for Determining the Elastic General-Instability Pressures of Ring-Stiffened Cylinders," David Taylor Model Basin Report 1570 (Jan 1962).
5. Kendrick, S., "The Buckling under External Pressure of Circular Cylindrical Shells with Evenly Spaced Equal Strength Circular Ring Frames-Part III," Naval Construction Research Establishment Report R244 (Sep 1953).



INITIAL DISTRIBUTION

Copies		Copies	
12	CHBUSHIPS	1	SUPSHIP, NNS
	2 Sci & Res Sec (Code 442)	1	NNSB & DD Co
	1 Lab Mgt (Code 320)	1	SUPSHIP, Pascagoula
	3 Tech Lib (Code 210L)	1	Ingalls Shipbldg Corp
	1 Applied Sci Br (Code 342)	1	Dir Def R & E, Attn: Tech Lib
	1 Prelim Des Br (Code 420)	1	CO, USNROTC & NAVADMINU, MIT
	1 Hull Des Br (Code 440)	1	O in C, PGSCOL, Webb
	1 Struc Sec (Code 443)	1	Dr. E. Wenk, Jr., Library of Congress
	1 Matls & Chem (Code 634)	1	Dr. R. C. DeHart, SW Res Inst
	1 Polymer, Fiber & Packaging Sec (Code 634C)	1	Prof. J. Kempner, Polytech Inst of Bklyn
3	CHONR	1	Dean V. L. Salerno, Fairleigh Dickinson Univ
	1 Res Coordinator (Code 104)	1	S. Kendrick
	1 Struc Mech Br (Code 439)		Naval Construction Res Est
	1 Undersea Prog (Code 466)		St. Leonard's Hill
2	CNO		Dunfermline, Scotland
	1 Undersea Warfare & AE Sec (Ap 702C)		
	1 Tech Anal & Advis Gr (Ap 07TB)		
1	CHBUWEPS (RRMA-3)		
1	CHBUDOCKS, (C-423)		
1	CO & DIR, USNEL		
1	CO & DIR, USNUL		
2	CDR, USNOL		
	1 WM Div		
2	DIR, USNRL		
	1 (Code 2027)		
	1 (Code 6210)		
1	CDR, USNOTS, China Lake		
1	CO, USNUOS, Newport		
20	CDR, DDC		
1	NAVSHIPYD P'TSMH		
1	NAVSHIPYD MARE		
1	NAVSHIPYD CHASN		
1	NAVSHIPYD NYK		
1	SUPSHIP, Groton		
1	EB Div, Gen Dyn Corp		





<b>DOCUMENT CONTROL DATA - R&amp;D</b>		
<i>(Security classification of title, body of abstract and indexing annotation must be entered when the overall report is classified)</i>		
1 ORIGINATING ACTIVITY (Corporate author)  David Taylor Model Basin		2 a. REPORT SECURITY CLASSIFICATION  Unclassified
		2 b GROUP
3 REPORT TITLE  THE EFFECT OF INTERMEDIATE HEAVY FRAMES ON THE ELASTIC GENERAL-INSTABILITY STRENGTH OF RING-STIFFENED CYLINDERS UNDER EXTERNAL HYDROSTATIC PRESSURE		
4. DESCRIPTIVE NOTES (Type of report and inclusive dates)  Final		
5. AUTHOR(S) (Last name, first name, initial)  Blumenberg, William F.		
6. REPORT DATE  January 1965	7a. TOTAL NO. OF PAGES  27	7b. NO. OF REFS  15
8a. CONTRACT OR GRANT NO.	9a. ORIGINATOR'S REPORT NUMBER(S)  1844	
b. PROJECT NO. S-F013 03 02		
c Task 1952	9b. OTHER REPORT NO(S) (Any other numbers that may be assigned this report)	
d.		
10. AVAILABILITY/LIMITATION NOTICES  Foreign announcement and dissemination of this report by DDC is not authorized.		
11 SUPPLEMENTARY NOTES	12. SPONSORING MILITARY ACTIVITY  Bureau of Ships	
13 ABSTRACT  Twenty-four machined models were collapsed under external hydrostatic pressure to evaluate the effect of intermediate heavy frames on the elastic general-instability strength of ring-stiffened cylinders. The models were designed with various overall lengths, heavy-frame spacings, and heavy-frame sizes; the cylinder diameter, the shell thickness, and the typical-stiffener size and spacing were held constant. The test results indicate that the effectiveness of a particular size of intermediate heavy frame decreases as the cylinder is lengthened at least to six diameters and also that the minimum size of heavy frames necessary to localize the failure between the heavy frames is possibly not dependent upon their spacing.  The values predicted by available analytical solutions show poor agreement with experimental results, whereas an existing empirical heavy-frame formula and a formula presented herein show better correlation.		

14. KEY WORDS	LINK A		LINK B		LINK C	
	ROLE	WT	ROLE	WT	ROLE	WT
External hydrostatic pressure Ring-stiffened cylinders Intermediate heavy frames Elastic general-instability strength						

INSTRUCTIONS

1. **ORIGINATING ACTIVITY:** Enter the name and address of the contractor, subcontractor, grantee, Department of Defense activity or other organization (*corporate author*) issuing the report.
- 2a. **REPORT SECURITY CLASSIFICATION:** Enter the overall security classification of the report. Indicate whether "Restricted Data" is included. Marking is to be in accordance with appropriate security regulations.
- 2b. **GROUP:** Automatic downgrading is specified in DoD Directive 5200.10 and Armed Forces Industrial Manual. Enter the group number. Also, when applicable, show that optional markings have been used for Group 3 and Group 4 as authorized.
3. **REPORT TITLE:** Enter the complete report title in all capital letters. Titles in all cases should be unclassified. If a meaningful title cannot be selected without classification, show title classification in all capitals in parenthesis immediately following the title.
4. **DESCRIPTIVE NOTES:** If appropriate, enter the type of report, e.g., interim, progress, summary, annual, or final. Give the inclusive dates when a specific reporting period is covered.
5. **AUTHOR(S):** Enter the name(s) of author(s) as shown on or in the report. Enter last name, first name, middle initial. If military, show rank and branch of service. The name of the principal author is an absolute minimum requirement.
6. **REPORT DATE:** Enter the date of the report as day, month, year; or month, year. If more than one date appears on the report, use date of publication.
- 7a. **TOTAL NUMBER OF PAGES:** The total page count should follow normal pagination procedures, i.e., enter the number of pages containing information.
- 7b. **NUMBER OF REFERENCES:** Enter the total number of references cited in the report.
- 8a. **CONTRACT OR GRANT NUMBER:** If appropriate, enter the applicable number of the contract or grant under which the report was written.
- 8b, 8c, & 8d. **PROJECT NUMBER:** Enter the appropriate military department identification, such as project number, subproject number, system numbers, task number, etc.
- 9a. **ORIGINATOR'S REPORT NUMBER(S):** Enter the official report number by which the document will be identified and controlled by the originating activity. This number must be unique to this report.
- 9b. **OTHER REPORT NUMBER(S):** If the report has been assigned any other report numbers (*either by the originator or by the sponsor*), also enter this number(s).
10. **AVAILABILITY/LIMITATION NOTICES:** Enter any limitations on further dissemination of the report, other than those

imposed by security classification, using standard statements such as:

- (1) "Qualified requesters may obtain copies of this report from DDC."
- (2) "Foreign announcement and dissemination of this report by DDC is not authorized."
- (3) "U. S. Government agencies may obtain copies of this report directly from DDC. Other qualified DDC users shall request through \_\_\_\_\_."
- (4) "U. S. military agencies may obtain copies of this report directly from DDC. Other qualified users shall request through \_\_\_\_\_."
- (5) "All distribution of this report is controlled. Qualified DDC users shall request through \_\_\_\_\_."

If the report has been furnished to the Office of Technical Services, Department of Commerce, for sale to the public, indicate this fact and enter the price, if known.

11. **SUPPLEMENTARY NOTES:** Use for additional explanatory notes.
12. **SPONSORING MILITARY ACTIVITY:** Enter the name of the departmental project office or laboratory sponsoring (*paying for*) the research and development. Include address.
13. **ABSTRACT:** Enter an abstract giving a brief and factual summary of the document indicative of the report, even though it may also appear elsewhere in the body of the technical report. If additional space is required, a continuation sheet shall be attached.

It is highly desirable that the abstract of classified reports be unclassified. Each paragraph of the abstract shall end with an indication of the military security classification of the information in the paragraph, represented as (TS), (S), (C), or (U).

There is no limitation on the length of the abstract. However, the suggested length is from 150 to 225 words.

14. **KEY WORDS:** Key words are technically meaningful terms or short phrases that characterize a report and may be used as index entries for cataloging the report. Key words must be selected so that no security classification is required. Identifiers, such as equipment model designation, trade name, military project code name, geographic location, may be used as key words but will be followed by an indication of technical context. The assignment of links, roles, and weights is optional.

MIT LIBRARIES

DUPL



3 9080 02753 0275

Date Due

JAN 25 2006

Lib-26-67

AUG 17 1977

OCT 7 1980